

INVESTIGATING THE EFFECTS OF CHANNEL ASPECT RATIO ON FLUID FLOW AND HEAT TRANSFER IN ABSORBER PLATES WITH MINICHANNELS

Oyinlola, M.A.,* Shire, G.S.F., Moss, R.W. and Khaliji Oskouei, M.

*Author for correspondence

School of Engineering,
 University of Warwick,
 Coventry, CV4 7AL,
 United Kingdom,

E-mail: M.A.Oyinlola@Warwick.ac.uk

ABSTRACT

This study experimentally investigates the fluid flow and heat transfer in two solar thermal absorber plates for compact (thin and light-weight) solar thermal collectors. Two metal plates with 270 mm long, 0.5 mm deep mini-channels having aspect ratios of 1 and 4 were studied. Constant heat flux, forced convection experiments were performed using Tyfocor® LS (a propylene glycol-based heat transfer fluid for thermal solar systems) at various flow rates and temperatures. Reynolds numbers were in the range 5-200. Measured Nusselt numbers were much lower than classical theory and were observed to be directly proportional to the product of the Reynolds number and Prandtl number (RePr). The plate with rectangular channels produced slightly higher Nusselt numbers and much lower pressure drops, making them a preferred option for this application.

INTRODUCTION

This paper investigates the thermal and hydraulic performance of two solar thermal mini-channel absorber plates for compact (thin and light-weight) solar thermal collectors. The proposed collectors will be an architecturally attractive option for incorporation in buildings and have the potential for improved thermal performance.

Mini- micro scale heat transfer and fluid flow has been extensively studied over the past 3 decades, for example [1-3], but this was largely in the context of micro-electronic components; there have been relatively few studies focused on micro-channel solar absorber plates. Sharma and Diaz [4] are some of the few researchers who have published studies on solar collectors based on mini-channels; they modelled an evacuated tube collector based on mini-channels. Oyinlola and Shire [5] showed that absorber plates with mini-channels, instead of the conventional arrangement, were a viable option for compact solar collectors. This paper further studies the use

of mini-channels in absorber plates; it investigates the effects of the channel aspect ratio (AR) while keeping the depth constant.

NOMENCLATURE

a	[m]	Channel Depth
b	[m]	Channel Width
C_p	[J/kg.°C]	Specific Heat Capacity
D_h	[m]	Hydraulic Diameter
f	[-]	Friction Factor
h	[W/m ² .°C]	Heat Transfer Coefficient
k	[W/m.°C]	Thermal Conductivity
L	[m]	Length of Channel
\dot{m}	[kg/s]	Mass Flow Rate
N_c	[-]	Number of Channels on Plate
Nu	[-]	Nusselt Number
Pr	[-]	Prandtl Number
Q	[W]	Heat supplied by Heater Mat
Re	[-]	Reynolds Number
S	[m ²]	Heat Transfer Surface Area
T	[°C]	Temperature
ρ	[kg/m ³]	Density
ω	[-]	Uncertainty
μ	[Pa.s]	Dynamic Viscosity

Subscripts

f	Fluid
in	Inlet
i	Plate Location
Out	Outlet
p	Plate

EXPERIMENTAL SETUP

The test rig was made up of two 340 × 240 × 10 mm aluminum slabs – a “top” and “bottom” piece. The plate to be tested (3 mm thick) was sandwiched between them. This arrangement allowed various plates to be tested without each

needing its own inlet and outlet connections. Figure 1 shows a picture of the two plates tested in this study. Three self-adhesive heater mats were stuck onto the top slab and provided a total heat flux of about 350 Watts. The rig was insulated with a custom-built Polyisocyanurate (PIR) box. Type T thermocouples, were stuck on the absorber plate. Further details of the test rig and the thermocouple arrangement can be seen in figure 2a and figure 2b respectively, figure 3 shows a cross section of the test rig.

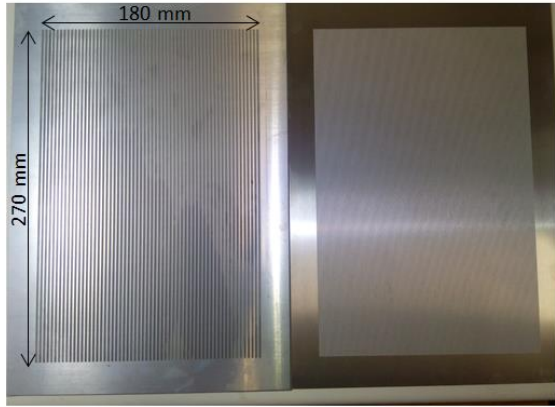


Figure 1 Plate with channel Aspect Ratio= (a) 4 (b) 1



Figure 2 (a) Test Rig (b) Thermocouple arrangement on Plate

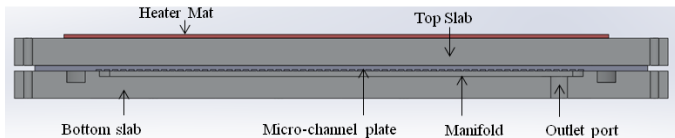


Figure 3 Cross section of test rig

The absorber plate with $AR = 4$ had 60 mini-channels $0.5 \text{ mm} \times 2 \text{ mm} \times 270 \text{ mm}$ long, while the other had 180 mini-channels $0.5 \text{ mm} \times 0.5 \text{ mm} \times 270 \text{ mm}$ long. The thermal working fluid was Tyfocor® LS, a propylene glycol-based heat transfer fluid for solar collectors. This was supplied at constant temperature and flow rate by a temperature controlled circulating bath. The fourth side of the channel was formed by the bottom piece that was clamped in place hard against the inter-passage ribs. Table 1 shows the different conditions that

the experiments were run at. The Reynolds number from all flow rates suggests laminar flow.

Table 1: The temperatures and flow rates used for the experiment

T_{in} (°C)	\dot{m}_1 (g/s)	\dot{m}_2 (g/s)	\dot{m}_3 (g/s)	\dot{m}_4 (g/s)	\dot{m}_5 (g/s)	\dot{m}_6 (g/s)	\dot{m}_7 (g/s)
5	2.0	3.5	4.8	5.4	7.9	9.9	12.3
20	2.2	4.4	6.5	9.2	11.2	14.2	16.5
40	3.4	6	9.6	12.1	14.8	17.6	20.7
60	4.9	8.2	10.9	13.8	16.7	19.4	22.2

Temperatures of the plate at different points (T_{pi}) as well as the inlet (T_{in}) and outlet (T_{out}) fluid temperatures were measured. The flow rate (\dot{m}) and pressure drop (Δp) were measured using a Coriolis mass flow meter and a differential pressure sensor respectively. The inlet and outlet temperature probes were placed after elbow fittings (for fluid mixing) to allow accurate readings of bulk fluid temperature. All the measured quantities were logged with a 16-bit National Instruments data acquisition system via Labview. Thermocouples were connected through a SCXI-1102 thermocouple interface board. Signals were sampled at 2 Hz, without any analogue filtering. At a given flow rate, the temperatures reached steady state after approximately 10–15 minutes. The power consumed by the heater mats was measured using a watt meter; these values were similar to the enthalpy change of the fluid between inlet and outlet. Figure 4 and 5 respectively show the schematic of the experimental setup and the actual apparatus.

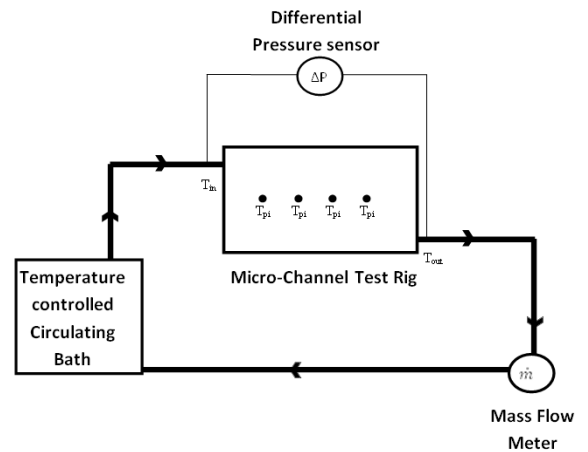


Figure 4 schematic of experimental setup

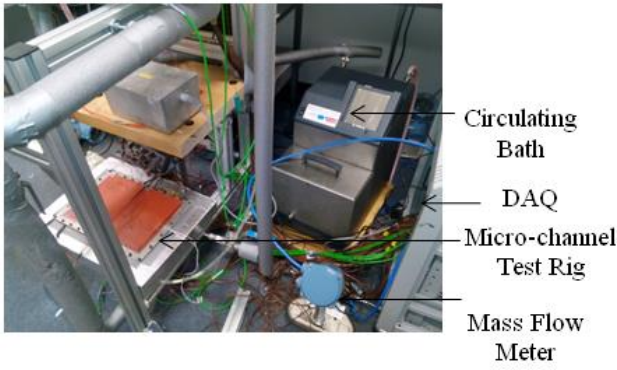


Figure 5 Actual experimental setup

UNCERTAINTY

The Data Acquisition system has a function for calibrating all channels. This procedure compensates for the inaccuracies in the whole measurement system. The temperature probes were bonded together, put in the bath and calibrated at a number of temperatures to match bath temperature readout. Voltages from the mass flow meter were calibrated to match its display readout while the differential pressure sensor was calibrated to match a hand held manometer.

After calibration, the maximum deviation observed in each sensor was taken as the instrument's uncertainty; this value was less than 0.1 K in the thermocouples. The observed maximum deviations were used to estimate the uncertainties in the calculated values, assuming that the deviations in each term were uncorrelated. For example, equations 1 and 2 [6] were used to estimate the uncertainty in the heat transfer coefficient and the friction factor. In both cases, the uncertainty was less than 15 %.

$$\omega_h = h \left[\left(\frac{\omega_Q}{Q} \right)^2 + \left(\frac{\omega_A}{A} \right)^2 + \left(\frac{\omega_{\Delta T_{pf}}}{\Delta T_{pf}} \right)^2 \right]^{1/2} \quad (1)$$

$$\omega_f = f \left[\left(\frac{\omega_{D_h}}{D_h} \right)^2 + \left(\frac{\omega_{\Delta p}}{\Delta p} \right)^2 + \left(\frac{\omega_\rho}{\rho} \right)^2 + \left(\frac{\omega_L}{L} \right)^2 + 2 \left(\frac{\omega_v}{v} \right)^2 \right]^{1/2} \quad (2)$$

RESULTS AND DISCUSSION

Equations 3 – 9 show the calculations used for analysing the results.

$$\text{Reynolds number, } Re = \left(\frac{\dot{m}}{abN_c} \right) \frac{D_h}{\mu} \quad (3)$$

$$\text{Mean plate temperature, } T_p = \frac{\sum_{i=1}^n T_{pi}}{n} \quad (4)$$

$$\text{Mean fluid temperature, } T_f = \frac{T_{in} + T_{out}}{2} \quad (5)$$

$$\text{Surface Area, } S = 2N_c L(a + b) \quad (6)$$

$$\text{Heat transfer coefficient, } h = \frac{Q}{S(T_p + T_w)} \quad (7)$$

$$\text{Nusselt number, } Nu = \frac{hD_h}{k} \quad (8)$$

Friction factor,

$$f = \frac{\Delta p}{\frac{1}{2} \rho v^2 \left(\frac{L}{D} \right)} = \Delta p \frac{D_h}{L} \frac{1}{\frac{1}{2} \rho \left(\frac{\dot{m}}{N_c ab} \right)^2} \quad (9)$$

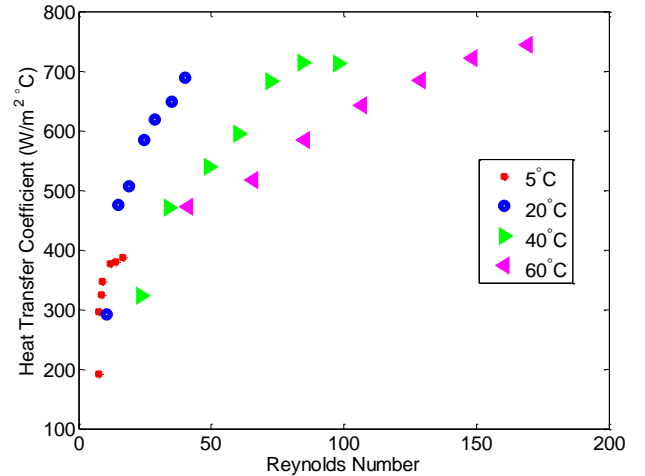


Figure 6 Heat transfer coefficient vs Reynolds number for 0.5 mm × 0.5 mm channels

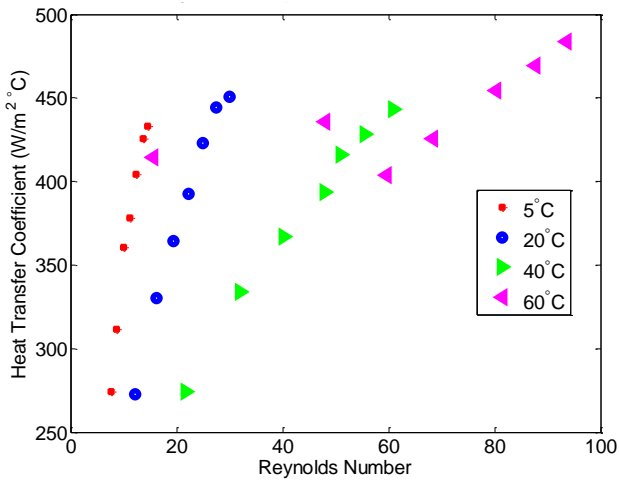


Figure 7 Heat transfer coefficient vs Reynolds number for $2\text{ mm} \times 0.5\text{ mm}$ channels

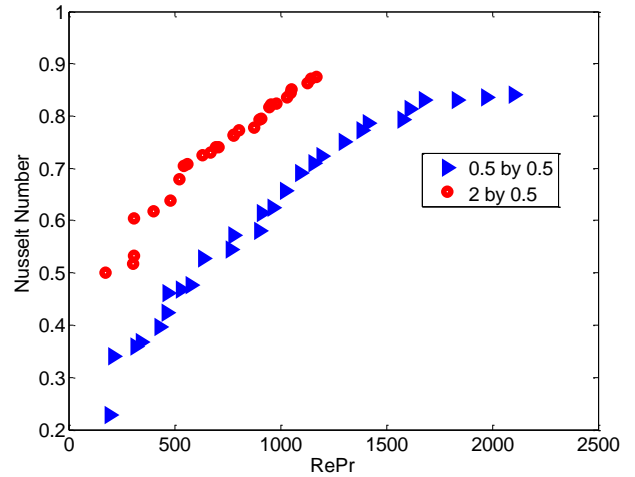


Figure 8 Nusselt number Vs product of Reynolds and Prandtl numbers

Thermal Performance

Figure 6 and 7 show plots of the heat transfer coefficient versus Reynolds number at the 4 inlet fluid temperatures for the $0.5\text{ mm} \times 0.5\text{ mm}$ and $2\text{ mm} \times 0.5\text{ mm}$ channels respectively; it can be observed that both plates have a similar trend of increasing heat transfer coefficient with the Reynolds number. The curves in both figures shift to the right as the temperature increases; this shows a significant influence of Prandtl number. The heat transfer coefficient are converted to the non-dimensional parameter, Nusselt number (Nu), and plotted against the product of the Reynolds number and Prandtl number (RePr) as shown in figure 8. This figure differs from the expected horizontal curves for Nusselt number in laminar flow but shows a direct relationship of Nu with RePr, a relationship synonymous with turbulent flow heat transfer correlation. This dependence of Nusselt number on Reynolds number has been achieved by several researchers, for example, [7, 8]. The measured Nusselt numbers are much lower than classical theory, [8-11] also reported this trend. Figure 10 compares the results of this study to the correlation by Peng and Peterson [10] and Choi, et al. [11]. The measured Nusselt numbers are scattered between this two correlations. Several explanations have been given for this, for example, the Birkman number [12], surface roughness[13], etc. Further investigations are being carried out to study the causes of this trend.

Figure 9 shows a plot comparing the heat transfer coefficient in both plates, at fluid inlet temperature of 20°C . These figures show that the $0.5\text{ mm} \times 0.5\text{ mm}$ channels (which have a hydraulic diameter of 0.5 mm), produce higher heat transfer coefficients than the $2\text{ mm} \times 0.5\text{ mm}$ channels (which have a hydraulic diameter of 0.8 mm). This was expected as smaller hydraulic diameters were expected to produce higher heat transfer coefficients as a result of the high contact surface area with the fluid. The relationship between the aspect ratio and the Nusselt number can be observed; channels with aspect ratio of 4 had slightly higher Nusselt numbers than channels with aspect ratio of 1.

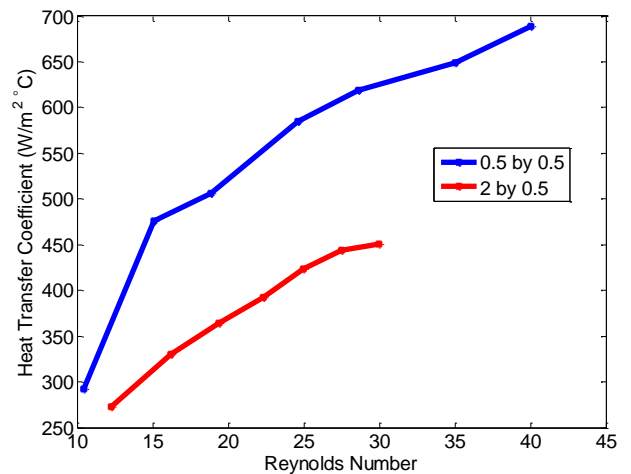


Figure 9 Heat transfer coefficient vs Reynolds number at $T_{in} = 20^\circ\text{C}$

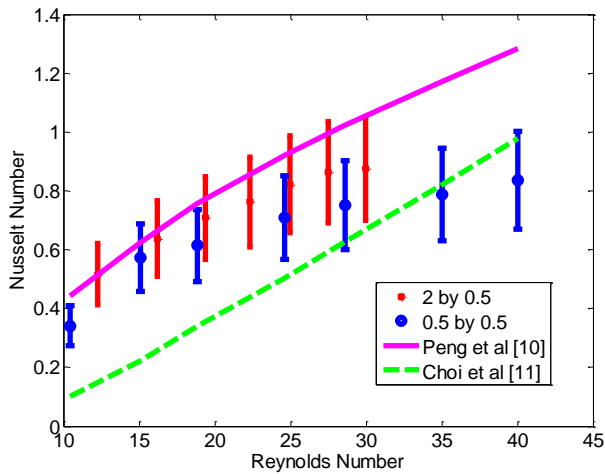


Figure 10 Heat transfer coefficient vs Reynolds number at $T_{in} = 40^{\circ}\text{C}$

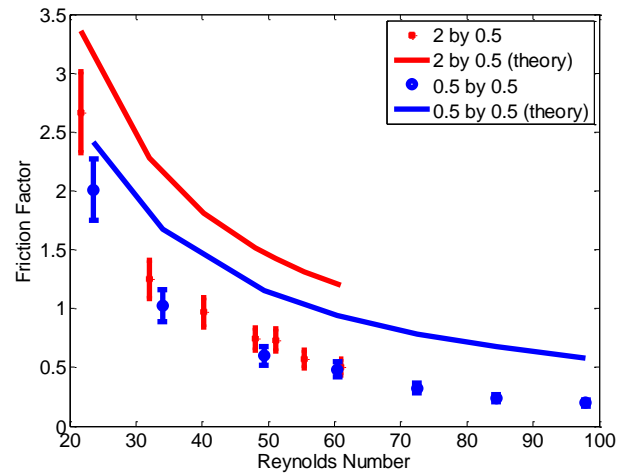


Figure 12 Friction factor vs. Reynolds number

Hydraulic Performance

Figure 11 shows the recorded pressure drop per channel for the two plates at inlet fluid temperature of 20°C . Higher pressure drops were recorded in the $0.5\text{ mm} \times 0.5\text{ mm}$ channels; this was expected as increased surface area implies increased frictional forces. Figure 12 shows a plot of measured friction factors against the Reynolds number. The measured friction factors are less than the expected relationship of $56.92/\text{Re}$ and $72.92/\text{Re}$ [14] for laminar flow in aspect ratio of 1 and 4 respectively.

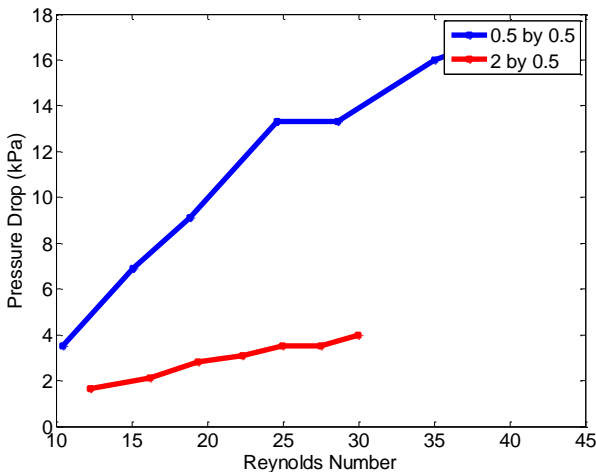


Figure 11 Pressure drop vs Reynolds number at $T_{in} = 20^{\circ}\text{C}$

CONCLUSION

The effects of channel aspect ratio on the thermal and hydraulic performance have been studied. Two plates with mini-channels having the same depth but different aspect ratios were investigated. The results show that the Nusselt number is a function of the product of the Reynolds and Prandtl numbers; measured Nusselt numbers were close to the predictions of [10, 11]. The rectangular channels had slightly better thermal performance and a much better hydraulic performance making them a preferred option for this application.

REFERENCES

- [1] Adams, T. M., Abdel-Khalik, S. I., Jeter, S. M., and Qureshi, Z. H., "An experimental investigation of single-phase forced convection in microchannels," *International Journal of Heat and Mass Transfer*, vol. 41, pp. 851-857, 1998.
- [2] Lee, P.-S., Garimella, S. V., and Liu, D., "Investigation of heat transfer in rectangular microchannels," *International Journal of Heat and Mass Transfer*, vol. 48, pp. 1688-1704, 2005.
- [3] Dogruoz, M. B., Arik, M., and Pautsch, A., "Heat transfer in microchannels: substrate effects and cooling efficiency for rectangular and circular ducts," in *Thermal and Thermomechanical Phenomena in Electronic Systems (ITherm), 2010 12th IEEE Intersociety Conference on*, 2010, pp. 1-7.
- [4] Sharma, N. and Diaz, G., "Performance model of a novel evacuated-tube solar collector based on minichannels," *Solar Energy*, vol. 85, pp. 881-890, 2011.
- [5] Oyinlola, M. A. and Shire, G. S. F., "Investigating Heat Transfer in Absorber Plates with Minichannels," in *13th UK Heat Transfer Conference (UKHTC13)*, London, 2013, pp. 740-747.
- [6] Holman, J. P., *Experimental methods for engineers*. Boston: McGraw-Hill/Connect Learn Succeed, 2012.

- [7] Gao, P., Le Person, S., and Favre-Marinet, M., "Scale effects on hydrodynamics and heat transfer in two-dimensional mini and microchannels," *International Journal of Thermal Sciences*, vol. 41, pp. 1017-1027, 11// 2002.
- [8] Hetsroni, G., Gurevich, M., Mosyak, A., and Rozenblit, R., "Drag reduction and heat transfer of surfactants flowing in a capillary tube," *International Journal of Heat and Mass Transfer*, vol. 47, pp. 3797-3809, 8// 2004.
- [9] Dixit, T. and Ghosh, I., "Low Reynolds number thermo-hydraulic characterization of offset and diamond minichannel metal heat sinks," *Experimental Thermal and Fluid Science*, vol. 51, pp. 227-238, 11// 2013.
- [10] Peng, X. F. and Peterson, G. P., "Convective heat transfer and flow friction for water flow in microchannel structures," *International Journal of Heat and Mass Transfer*, vol. 39, pp. 2599-2608, 1996.
- [11] Choi, S. B., Barren, R. R., and Warrington, R. Q., "Fluid flow and heat transfer in micro-tubes," *ASME DSC* pp. 89-93, 1991.
- [12] Tso, C. P. and Mahulikar, S. P., "The use of the Brinkman number for single phase forced convective heat transfer in microchannels," *International Journal of Heat and Mass Transfer*, vol. 41, pp. 1759-1769, 6// 1998.
- [13] Qu, W., Mala, G. M., and Li, D., "Heat transfer for water flow in trapezoidal silicon microchannels," *International Journal of Heat and Mass Transfer*, vol. 43, pp. 3925-3936, 11/1/ 2000.
- [14] Çengel, Y. A. C. J. M., *Fluid mechanics : fundamentals and applications*. Boston, Mass. [u.a.]: McGraw-Hill, 2010.